LRP 416/90 October 1990

DC SPACE-CHARGE INDUCED FREQUENCY UP-SHIFT IN A QUASI-OPTICAL GYROTRON

S. Alberti, M.Q. Tran, T.M. Tran

DC space-charge induced frequency up-shift in a quasi-optical gyrotron

S. Alberti, M.Q. Tran, T.M. Tran
Centre de Recherches en Physique des Plasmas,
Association Euratom-Confédération Suisse,
Ecole Polytechnique Fédérale de Lausanne,
21, Av. des Bains, CH-1007 Lausanne,
Switzerland

Recent experiments on a 100GHz quasi-optical gyrotron have shown that for a large resonator set-up [1] the observed frequency up-shift between the starting current and a current of 10A corresponds to a shift of 4−5 longitudinal modes. In this Letter it is shown that the interpretation of this frequency up-shift should involve the current dependent electron beam voltage depression in the beam tunnel and the interaction region for both the single-mode and multi-mode time evolution codes.

For a given experimental set-up, the non-linear efficiency of a gyrotron oscillator can be described as a function of the beam current I_b and the detuning $\Delta\omega$ which is defined as the relative frequency mismatch between the emitted frequency ω and the relativistic cyclotron frequency Ω_0/γ_0, that is :

$$\frac{\Delta\omega}{\omega} = 1 - \frac{\Omega_0}{\gamma_0\omega} \,. \tag{1}$$

It has been shown [2] that the optimum detuning $\Delta\omega_{opt}$ which defines the maximum non-linear efficiency is an increasing function of the beam current I_b. In a cylindrical cavity gyrotron this optimum detuning can be experimentally controlled by adjusting the DC magnetic field because, both, the resonant frequency ω and the relativistic factor γ_0 are fixed. On the other hand, in the case of a quasi-optical gyrotron (QOG) which makes use of an open Fabry-Pérot resonator, the relatively high density of longitudinal modes ($TEM_{0,0,q} \quad ; q \simeq 220-230$), implies that the optimum detuning cannot be reached by tuning the DC magnetic field but has to be reached through the non-linear mode coupling which may shift the oscillation towards the higher frequency region. For the large resonator case of the 100GHz QOG described in Ref. 1, the experimentally observed frequency up-shift between the starting current and a beam current of 10A corresponds to 4–5 longitudinal modes where the mode separation is 444MHz. Similar observations have been made for the 120GHz QOG developed at NRL [3]. In order to explain these experimental observations, the current-dependent electron beam voltage depression in the beam tunnel and the interaction region has to be taken into account. In this Letter results of the simulation including the DC space-charge effects (beam depression) will be presented, both, for the single-mode and multi-mode models. A comparison with the experimental results is also made.

In order to compute the beam depression profile, $\Phi_b(r,z)$, let's consider an annular electron beam with inner and outer beam radius r_1 and r_2, respectively, and an interaction region modeled by a grounded conducting cylinder of diameter $2r_w$ (equal to the mirror separation d) and length L (equal to the distance between the upstream and downstream beam tunnels). The outer beam radius r_2 is assumed to be equal to the beam tunnel radius which which implies that the DC space-charge effects in the beam tunnels are neglected. The quantity $\Phi_b(r,z)$ can be derived making use of the Green function for the interior of a cylinder [4]:

$$\Phi_b(r,z) = n_0\left(\frac{32}{r_w^2}\right)\sum_{n=1}^{\infty}\sum_{k=0}^{\infty}\frac{\sin\left[\frac{(2k+1)\pi(z+L/2)}{L}\right]J_0\left(\frac{x_{0n}r}{r_w}\right)h(r_1,r_2,r_w)}{(2k+1)\left(\frac{x_{0n}}{r_w}\right)\left[\left(\frac{x_{0n}}{r_w}\right)^2+\left(\frac{(2k+1)\pi}{L}\right)^2\right]J_1^2(x_{0n})} \,, \tag{2}$$

where x_{0n} are the zero's of the ordinary Bessel function $J_0(x)$, $h(r_1,r_2,r_w)$ is a geometrical factor:

$$h(r_1, r_2, r_w) = r_2 J_1(\frac{x_{0n} r_2}{r_w}) - r_1 J_1(\frac{x_{0n} r_1}{r_w}) \quad (3)$$

and the charge density n_0 is assumed to be constant. By fixing n_0 it is obvious that the beam depression calculation is not self-consistent; however, for the electron beam densities considered here, this approximation only slightly underestimates the self-consistent results. A more self-consistent treatment of this problem has been worked out by T.C. Genoni [5]. A typical beam depression profile calculated for the parameters described in Table I, taken from Ref. 1, gives a maximum beam depression at the resonator center ($z = 0$) and outer beam radius ($r = r_2$) and is as high as 6.5kV for a beam current of 10A. The maximum beam depression as a function of beam radius r_2 and distance $L/2$ is in agreement with the approximated formula (27) of Ref. 3.

In order to take into account the DC space charge field $E_z = -\frac{\partial \Phi_b(r_2, z)}{\partial z}$ in the single-mode and multi-mode simulations, the following equation for the parallel momentum p_{zj} (normalized to mc) of an electron j:

$$\frac{dp_{zj}}{dz} = \frac{e}{mc^2} \frac{\gamma_j}{p_{zj}} \frac{\partial \Phi_b}{\partial z}, \quad (4)$$

where $\gamma_j = \sqrt{1 + p_{\perp j}^2 + p_{zj}^2}$ is the relativistic factor and $p_{\perp j}$ is the normalized perpendicular momentum, has been added to the usual particle equations [6]. Since the electron plasma frequency to cyclotron frequency ratio is very small ($\frac{\omega_p}{\Omega_c} \simeq 0.04$), it is possible to neglect the radial component of the DC space charge electric field. The resonator modes are the $TEM_{0,0,q}$ Gaussian modes. The detuning given by Eq. 1 is always computed using γ_0 at the beginning of the interaction region ($\gamma_0 = 1.135$).

In the simulation presented below, the beam and resonator properties are, respectively, those of table I of the present Letter and table II of Ref. 1. The results given by the single-mode equilibrium code are shown in Fig. 1. The RF power versus detuning at fixed currents, is shown for two cases: without beam depression (1a) and with beam depression (1b). The instability frequency band shifts towards the high frequencies due to the beam depression, but the maximum RF power remains almost the same, compared to the case without beam depression. For a given set of parameters the single-mode equilibrium model gives only the possible equilibrium points in the frequency-RF power space, but does not give any information about the accessibility of those points. The accessibility and the actual operating point can only be found by a multi-mode time evolution model. The numerical results of such a model are given by the multi-mode code and are shown in Figs. 2 and 3, presenting the detuning versus beam current and the RF power versus beam current respectively. Each figure shows two cases: without and with beam depression. From Fig. 2 it can be seen that the inclusion of the beam depression leads to a higher detuning as the current is increased. The continuous line is an estimate of the contribution to the detuning from the beam depression $\Delta\gamma$ based on the following relation:

$$\frac{\Delta\omega}{\omega_0} = -\frac{\Omega_0}{\omega_0\gamma_0}\frac{\Delta\gamma}{\gamma_0}, \tag{5}$$

where ω_0 is the emitted frequency at the starting current. The total detuning given by the multi-mode code roughly follows the line given by Eq. 5 but the interpretation of the detailed behavior is not straightforward since it depends on the non-linear mode coupling. In Fig. 3 the dashed line corresponds to the maximum (with respect to the detuning , see Fig. 1b) theoretical RF power calculated with the single-mode code. It should be noticed that in neither case, (without or with beam depression), can this maximum power be reached. This is a consequence of the fact that the optimum detuning $\Delta\omega_{opt}$ is not reached in either case.

A comparison of the experimental results with the theoretical predictions given by the multi-mode time evolution simulation code is given in Figs. 4 and 5, showing the same curves as in Figs. 2 and 3. In Fig. 4 a good agreement is found between theory and experiment if the beam depression is taken into account. In Fig. 5 the total measured RF power (including the second harmonic contribution and the output coupling efficiency of $\epsilon_c = 0.9$ [1]) follows more closely the curve including the space charge effect at high current.

Summarizing these results, it is observed that the experimental measurements are in agreement with the theory if the DC space charge effects are included; however, under our experimental conditions the optimum detuning condition is never reached. This limitation is due to the difficulty in controlling the detuning and could be solved, by controlling the detuning through a variation, in time, of the beam energy or the DC magnetic field (in a CW experiment) if the mode is stable. It has been verified by numerical computation that, for example, a change in the beam voltage V_b from 70 kV to 80 kV can drastically increase the output power and efficiency over that of the case in which 80kV is reached in one step [7]. Plans to implement such a scheme are under consideration.

Aknowledgments

We would like to thank Dr. T. Goodman for a critical reading of the manuscript.

[1]S. Alberti, M.Q. Tran, J.P. Hogge, T.M. Tran, A. Bondeson, P.Muggli, A. Perrenoud, B. Jödicke, and H.G. Mathews, Phys. Fluids B, **2**,1654 (1990).

[2]B.G. Danly and R.J. Temkin, Phys. Fluids,**29**,561 (1986).

[3]A.W. Fliflet, T.A. Hargreaves, W.M. Manheimer, R.P. Fischer, and M.L. Barsanti, IEEE Trans. Plasma Science,**18**,306 (1990).

[4]J.D. Jackson., *Classical Electrodynamics*, chapter 3, page 134. Wiley, New York, 1975.

[5]T.C. Genoni., J. Appl. Phys.,**51**, 3426 (1980).

[6]A. Bondeson, W.M. Manheimer, and E. Ott, Infrared and Millimeter Waves, **9**, 309 (1983).

[7]M.Q. Tran, To be published by the Institute of Applied Physics of Nijni Novgorod, USSR, in *Proceedings of the Int. workshop on Strong Microwave Plasma Interaction*, Suzdal, (1990).

FIG. 1. The RF power versus detuning for different beam currents I_b without SC fields (a) and with SC fields (b) obtained by a single-mode equilibrium code.

FIG. 2. Detuning versus beam current without SC fields (circles), and without (squares) calculated with a multi-mode time-evolution code. The continuous line indicates the contribution on the detuning given by the beam depression is obtained from formula (5).

FIG. 3. RF power versus beam current curves for the same two cases as in figure 2: without and with SC charge effects obtained from a multi-mode code. The dotted line is the maximum RF power obtained by a single-mode code.

FIG. 4. Comparison between theory and experiment of the detuning versus beam current.

FIG. 5. Comparison between theory and experiment of the total emitted power (including a coupling efficiency of $\epsilon_c = 0.9$) versus beam current. The open circle indicate the experimental points (second harmonic emission included [1]), the thin line and the thick line are respectively the theoretical results given by the multi-mode simulation for the two cases without and with SC fields.

TABLE I. Experimentally optimized beam properties at the entrance of the interaction region. Acceleration voltage, $V_b = 70$kV; mode-anode voltage, $V_a = 30$kV; beam current, $I_b = 10$A; and DC magnetic field, $B_0 = 3.96$T.

Inner beam radius r_1	1.86 mm
Outer beam radius r_2	2.14 mm
Length L	120 mm
Mirror separation d	320 mm
Mean perpendicular velocity $\langle\beta_\perp\rangle$	0.359
Perpendicular velocity deviation $\Delta\beta_\perp$	2.5 %
Mean parallel velocity $\langle\beta_\parallel\rangle$	0.308
Parallel velocity deviation $\Delta\beta_\parallel$	3.4 %
Mean pitch angle $\langle\alpha\rangle$	1.16
Pitch angle deviation $\Delta\alpha$	6 %
Mean relativistic factor $\langle\gamma_0\rangle$	1.135
Relativistic factor deviation $\Delta\gamma$	0.02 %
Plasma frequency to cyclotron frequency ratio $\frac{\omega_p}{\Omega_c}$	0.04

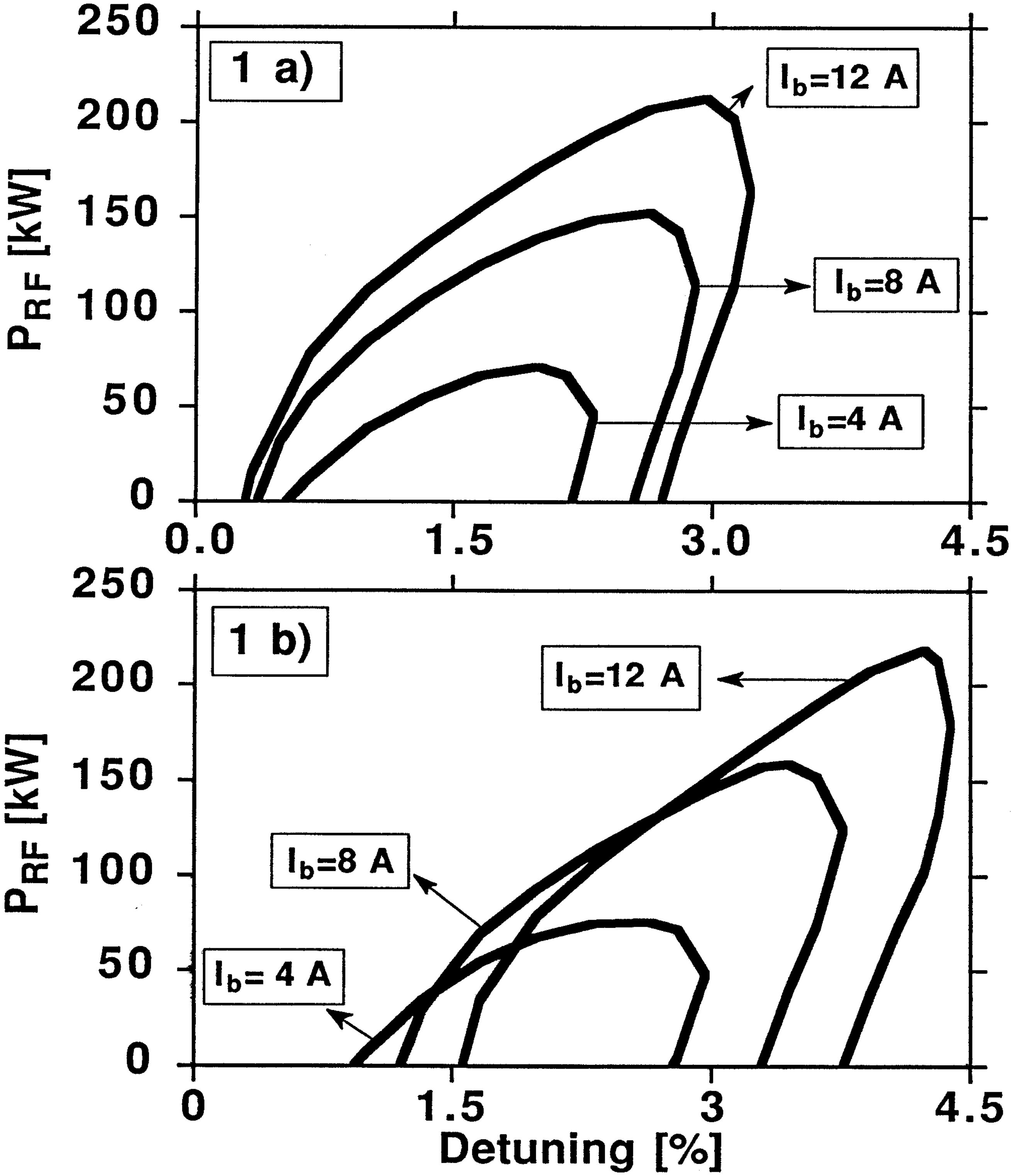
1 a)
1 b)
I_b=12 A
I_b=8 A
I_b=4 A
I_b= 4 A
P_{RF} [kW]
Detuning [%]
250
200
150
100
50
0
0.0
1.5
3.0
4.5
0
3

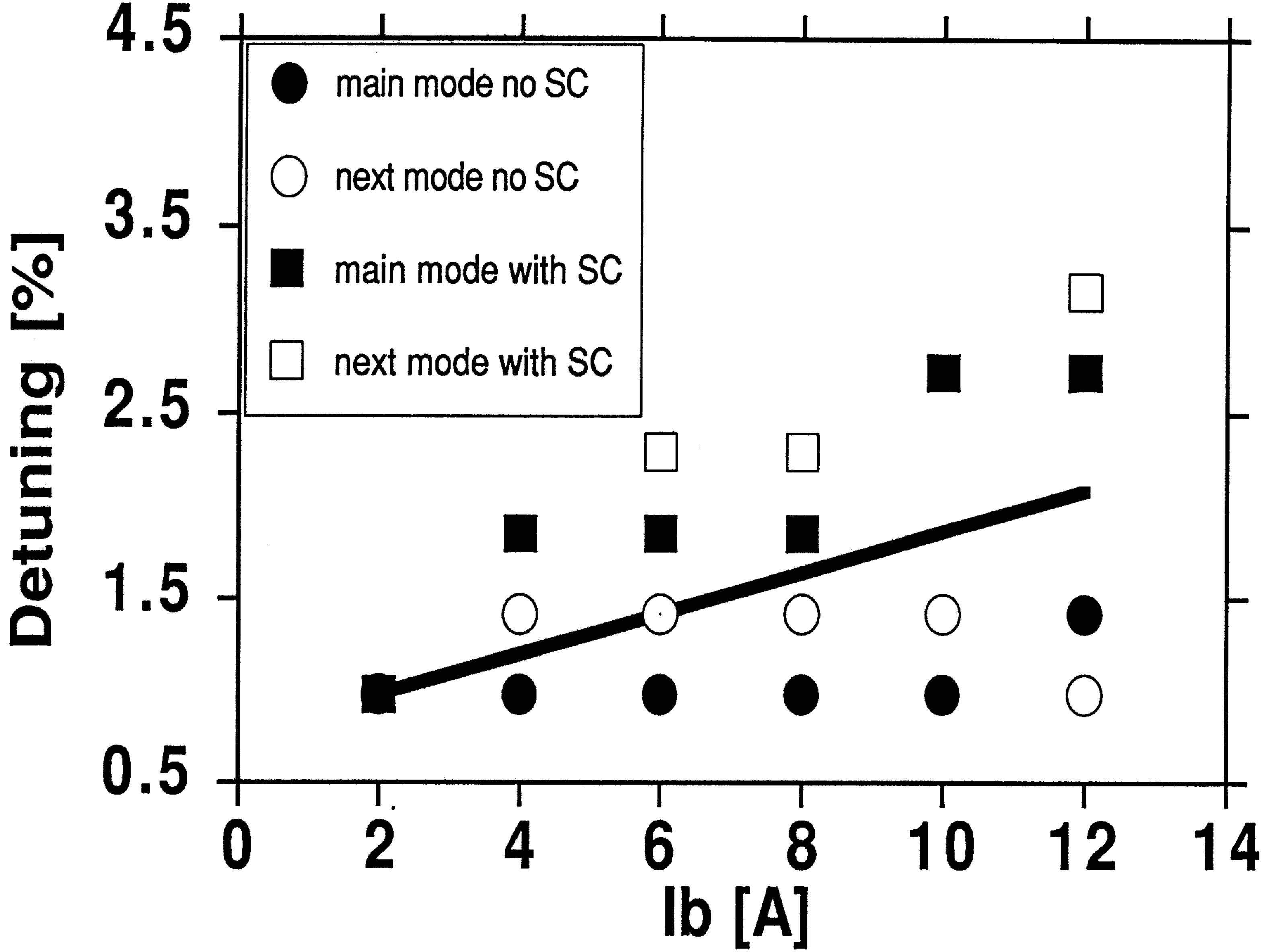
4.5
3.5
2.5
1.5
0.5
Detuning [%]
0
2
4
6
8
10
12
14
Ib [A]
main mode no SC
next mode no SC
main mode with SC
next mode with SC

Errata

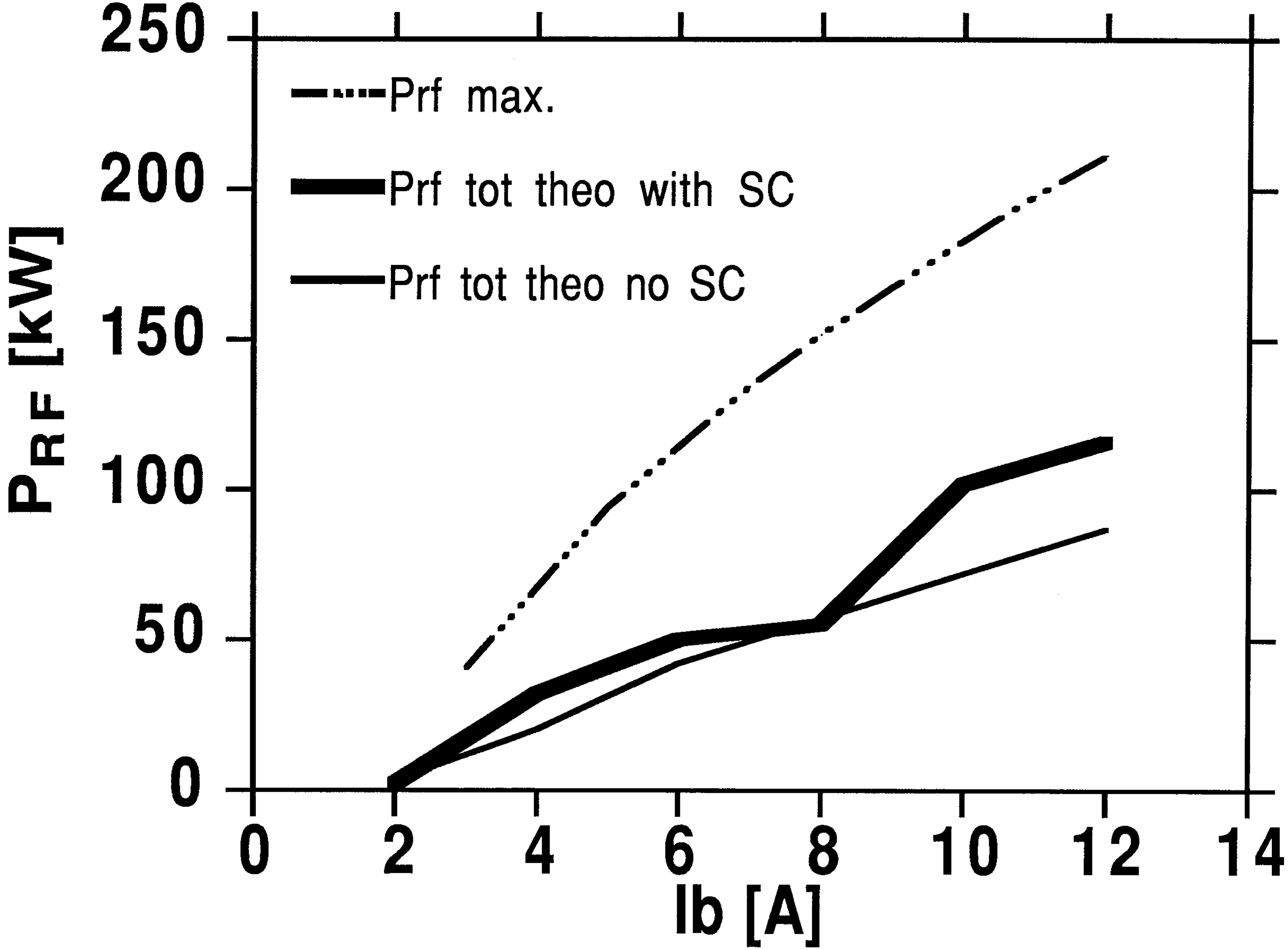

250
200
150
100
50
0
P_{RF} [kW]
0
2
4
6
8
10
12
14
Ib [A]
Prf max.
Prf tot theo with SC
Prf tot theo no SC

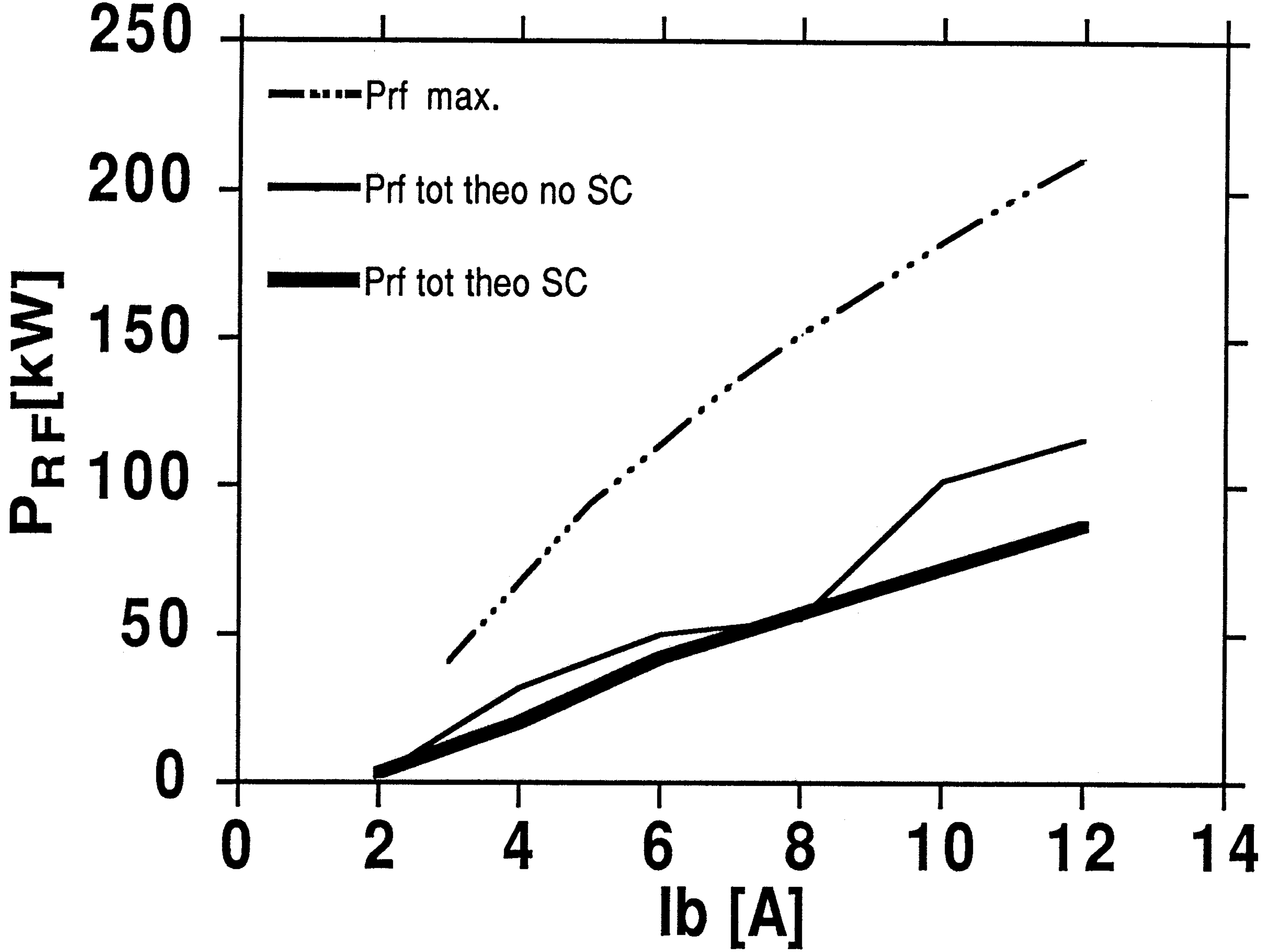

Prf max.
Prf tot theo no SC
Prf tot theo SC
250
200
150
100
50
0
P_{RF}[kW]
0
2
4
6
8
10
12
14
Ib [A]

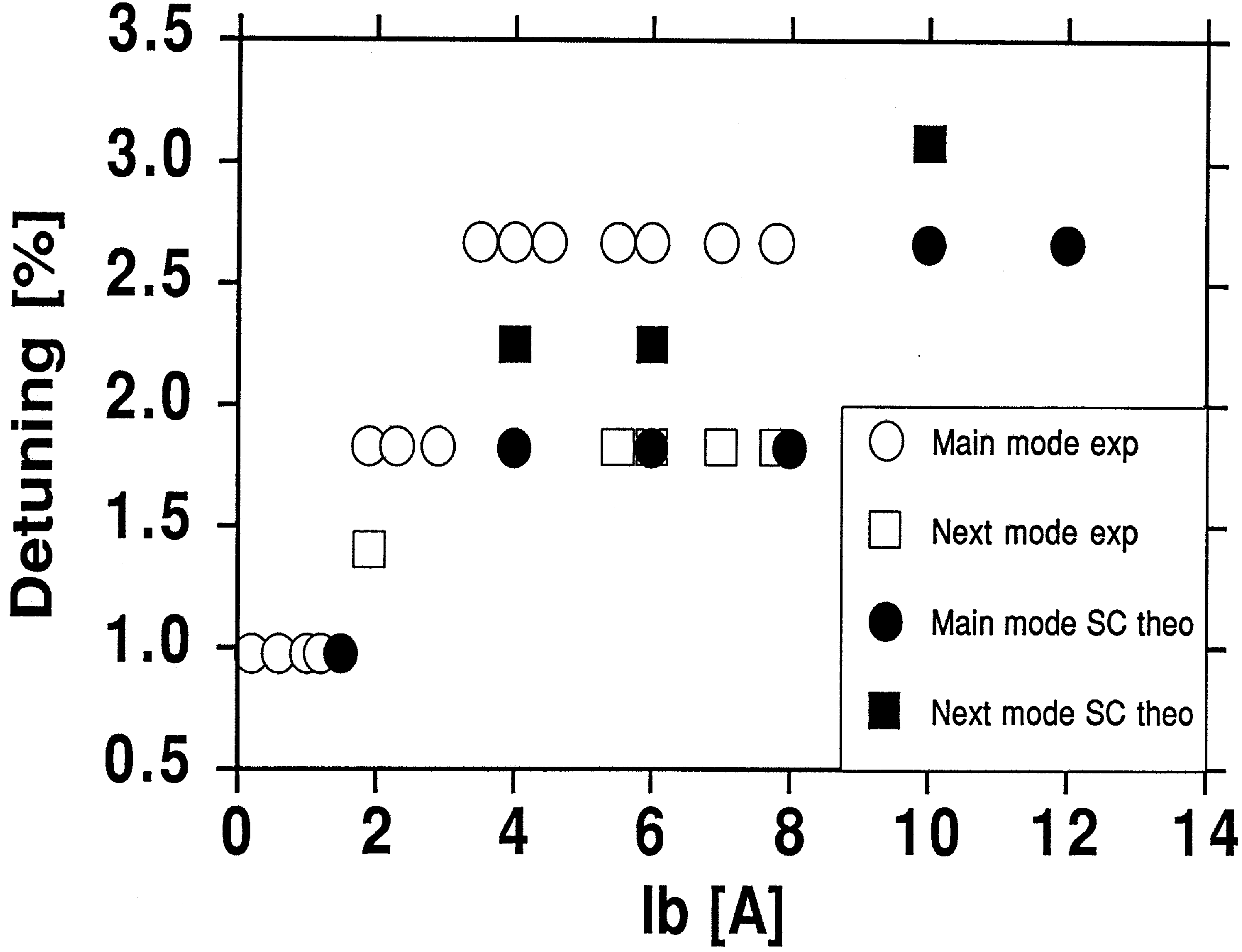
Detuning [%]
3.5
3.0
2.5
2.0
1.5
1.0
0.5
0
2
4
6
8
10
12
14
Ib [A]
Main mode exp
Next mode exp
Main mode SC theo
Next mode SC theo

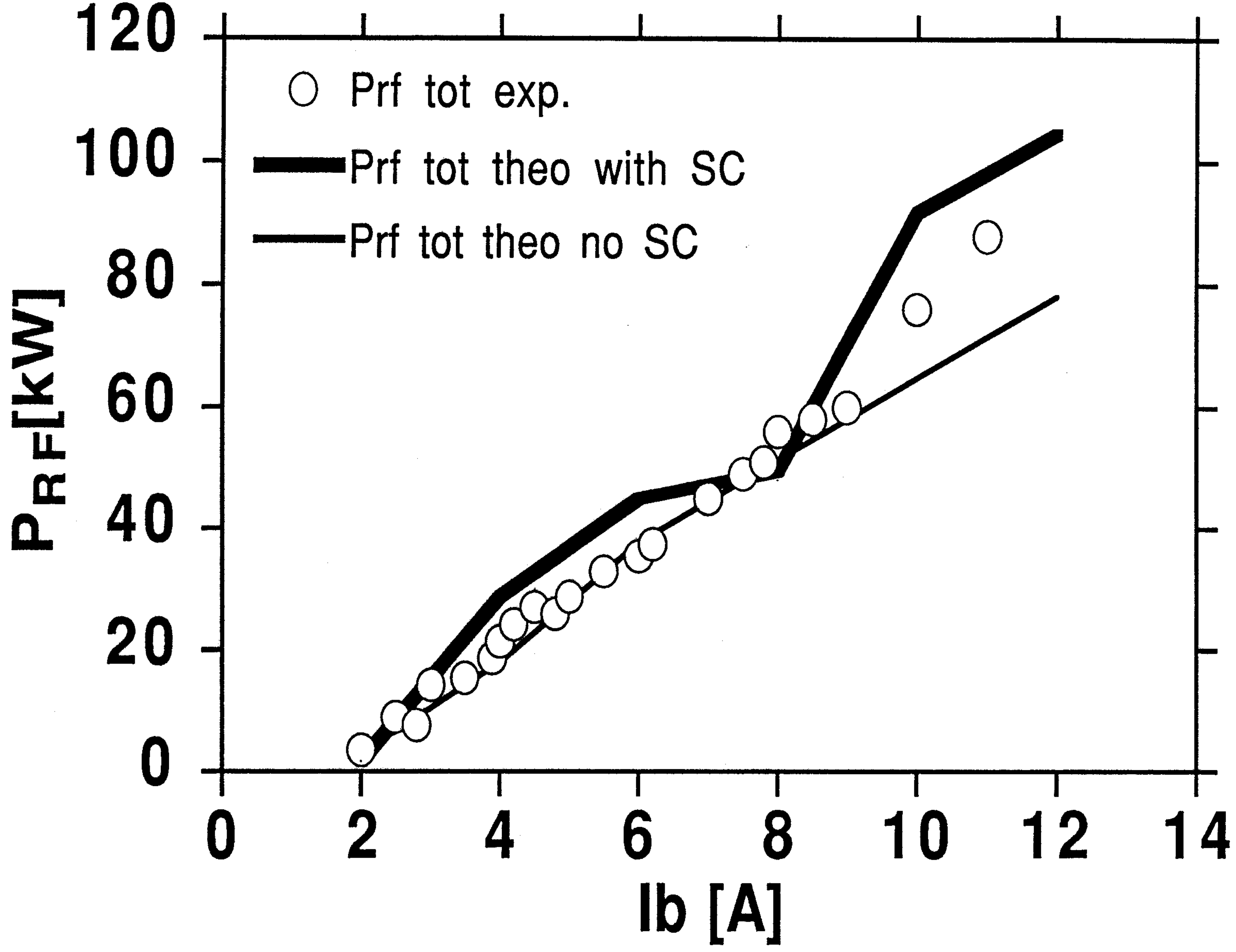
Prf tot exp.
Prf tot theo with SC
Prf tot theo no SC
P_RF[kW]
Ib [A]
0
20
40
60
80
100
120
0
2
4
6
8
10
12
14